MASTER THESIS

PRESSURE INSOLES FOR GAIT AND BALANCE ESTIMATION

Mohamed Irfan Mohamed Refai

BIOMEDICAL SIGNALS AND SYSTEMS
PROF. DR. IR. PETER H. VELTINK

EXAMINATION COMMITTEE
Dr. ir. Bert-Jan F. van Beijnum (Chair)
Prof dr. ir. Peter H. Veltink
Jaap H. Buurke, PhD, PT
Prof. dr. ir. H.F.J.M. Koopman (External)

DOCUMENT NUMBER
EWI-BSS – 17-01

17/02/2017

UNIVERSITY OF TWENTE.

ACKNOWLEDGEMENT

The window of my room in ZH 215 opens to an entrance of the UT. People swirl about like currents, some turbulence here, some linear flow there. I watch them pass by as it induces a sense of calm. A soothing scene that settles me down.

Sometimes, it transports me to the moment where it all began. People along the way that helped me come here, to the eventful window of ZH 215. Arno Stienen’s room looms into memory. In the summer of 2015, I spoke to him for a short summer project. One thing led to another, and I met Peter Veltink at the Biomedical Signals and Systems (BSS) who offered me choices. Choices that could rewrite my plans for the next few years. Choices that brought me to a meeting with Peter and Bert-Jan van Beijnum who were happy to offer me the NeuroCIMT project that would follow as a PhD. I thank you, Arno, Peter, and Bert-Jan for offering me these choices that brought me here.

Thank you once again Bert-Jan for being patient with my questions, and for reminding me that boundaries exist only so that we can push ahead. I love the discussions we have, that flow beyond focus. And I believe we have only started.

I would also like to acknowledge all my colleagues at the BSS, especially Angelos, Dirk, and Fokke who helped me setup the ForceShoes™, for their quick replies, and patient answers. And of course, one cannot complete a project at the BSS, if Ed and Marcel weren’t around for their lightning speed support. Thank you, guys!

A journey is not without confusions and forks. Decisions need to be made and formalities must be completed. Thank you, Sandra, for helping me through these hurdles at the BSS.

As humans, we are in constant need of true company and friendship. My comfy circle of friends has always helped me grapple with my weirdness and fluctuations. I thank you Ashwini, for agreeing to take on that responsibility forever.

I would like to acknowledge the pinky fingers that I have clutched on and have brought me this far. My parents, boulders that show me where the shore is. With them, I have been able to push myself so far. Thank you for being a silent, yet significant support.

Thank you all for pushing me so far. I still have a long way to go.

To a new beginning. Prost!

The most beautiful thing we can experience is the mysterious. It is the source of all true art and science.

- Albert Einstein

-

To my Parents; Rabiath Mam and Refai Sir.

CONTENTS

Article

Pressure Insoles for Gait and Balance Estimation

Mohamed Irfan Mohamed Refai [1,*], Bert-Jan F. van Beijnum [1], and Peter H. Veltink [1]

[1] Biomedical Signals and Systems, University of Twente
* Correspondence: m.i.mohamedrefai@utwente.nl; Tel.: +31-684-389-579

LaTeX template adapated from MDPI sensors

Abstract: Clinical therapy following stroke aims at tackling induced impairment in motor ability, gait, and balance. Once transferred home, remote monitoring of subject's performance is necessary for objective evaluation, improving mobility and preventing maladaptation. This requires a wearable and unobtrusive system capable of estimating ambulatory gait and dynamic balance measures, such as Extrapolated Centre of Mass (XCoM) and Dynamic Stability Margin (DSM). Currently, ForceShoes^{TM} (Xsens Technologies B.V., The Netherlands) had been developed for this purpose. However, it is bulky and conspicuous. As a lightweight and inconspicuous alternative, pressure insoles (medilogic® insoles, T&T medilogic Medizintechnik GmbH, Germany) coupled with IMUs, are investigated for objective quantification of gait and dynamic balance measures. Although, to obtain such measures, 3D forces and moments are required. Linear regression models were used to model 3D forces/moments from the 1D plantar pressures measured from pressure insoles. The predicted forces and moments were used for estimation of XCoM and DSM. These parameters were compared with the estimations done by the forces and moments from the ForceShoes^{TM}. High correlation and low differences between the estimations from predicted and measured forces and moments show that pressure insoles can indeed be used as an wearable alternative.

Keywords: Pressure Insoles; Gait Estimation; Dynamic Stability; Extrapolated Centre of Mass

1. Introduction

Occurrence of stroke cuts off nutrients to brain cells. This results in death of brain cells compromising motor functions causing poor recovery of activities of daily living, mobility, and balance. During rehabilitation, stroke survivors are trained to improve their motor functions to regain motor control and balance [1]. For a short overview on stroke, refer Appendix A.

Functional recovery includes aspects of behavioural restitution as well as behavioural substitution [2]. Behavioural restitution is the return towards intra-limb motor control on the affected side, whereas behavioural substitution is defined as the use of the unaffected limb to accomplish desired tasks. For instance, in functions of lower extremity, stroke survivors display inter-subject variability in gait patterns especially in step lengths, swing and stride time, when compared to healthy individuals [3]. Survivors could be therefore, trained towards behavioural restitution. Stroke survivors have also shown to have variability between the affected and non-affected leg [3]. This could be a manifestation of behavioural substitution. There exists a mixed consensus on the implementation of behavioural restitution or substitution training strategies [4].

Better understanding of recovery and the effect of restitution and substitution strategies can be obtained by assessment of the stroke survivor. Monitoring recovery during rehabilitation is feasible via clinical outcome measures, and instrumented laboratory facilities. Clinical outcomes indicate the change in capacity or functionality of given tasks whereas objective quantification using instrumented systems offers kinematic and kinetic changes in impairment level of said tasks [5].

Once the stroke survivor is discharged from the clinic, she/he is expected to continue functional training to maintain recovery. Physical therapy after discharge helps increase independence in activities of daily life and social interactions [6]. As instrumented laboratory facilities are expensive, wearables are needed for objective quantification while monitoring recovery.

ForceShoes^{TM} (Xsens Technologies B.V., Enschede, The Netherlands) had been developed as a wearable solution to monitor gait and dynamic balance [7,8]. The system measures acceleration and orientation of the feet and contact forces under it. ForceShoes^{TM} can offer holistic reconstruction of kinematics and kinetics of both feet during walking [9–11]. It has been validated against standard systems, such as force plates and motion capture, for measurement of contact forces and foot positions respectively [8,12,13]. Unlike these systems, ForceShoes^{TM} has the advantage of being portable, and not restricted by area of measurement setup or marker placement.

Gait measures such as step length, width and stride time can be estimated using Inertial Measurement Units (IMUs) on the ForceShoes^{TM}. IMUs consist of a accelerometer, gyroscope, and magnetometer. Acceleration and orientation information is fed to an Extended Kalman Filter to improve the accuracy of position and velocity estimation. Weenk et al., [8], reduced the drift in position estimation by using ultrasound range updates. These updates provide distance between the two feet periodically to the Extended Kalman Filter.

To study balance using ForceShoes^{TM}, Schepers et al., [9] derived Centre of Mass (CoM) using the 3D forces/moments sensors. Extrapolated Centre of Mass (XCoM) is the CoM along with the direction of walking. The trajectory of the XCoM projected on the ground with respect to the Base of Support (BoS) is an indication of dynamic stability [14]. BoS is the region between two feet in contact with the ground. If the XCoM is within the BoS, the person is said to be stable. However, if the XCoM is beyond the BoS, the person can be said to be unstable, unless the XCoM is directed towards the BoS [14]. Meulen et al., [10] used the shortest distance from the XCoM and the frontline of the BoS as a condition of stability during continuous walking, called as the Dynamic Stability Margin (DSM) [10]. The study shows that stroke survivors with a low score on the Berg Balance Scale (BBS) have a negative DSM and are hence, dynamically stable during walking. Using the above methods, the ForceShoes^{TM} can be used to objectively evaluate gait and dynamic balance of stroke subjects in an ambulatory or home setting.

However, the ForceShoes^{TM} are limited in their application as a wearable home system. The system is quite bulky, where each shoe weighs around 1 kg. The ForceShoes^{TM} look quite conspicuous and are higher than normal shoes. They cannot be integrated into every day use shoes due to the use of heavy sensors. Alternative sensor systems for ambulatory estimation can be achieved by using IMUs. However, reliance on the IMUs alone for a holistic estimation of kinetics and kinematics is not feasible due to issues of drift. Karatsidis et al, [15] showed the estimation of 3D forces and moments using 17 IMUs placed in a full body suit. This information can be used to estimate gait and dynamic balance. Though the results show good confidence in the estimation of 3D forces and moments, the system requires extensive setup. Further research is required for an alternative lightweight and inconspicuous method for ambulatory estimation of gait and dynamic balance.

Pressure insoles could be a suitable alternative. They can be slipped into everyday use shoes, are lightweight, and inconspicuous. They provide 1D plantar pressures under the feet during walking and can be used for estimating a range of gait parameters [16–18]. Further details on pressure insoles is given in Appendix B.

Pressure insoles can only provide the vertical 1D plantar pressure. A system consisting of pressure insoles and IMUs can replace the function of ForceShoes^{TM} in estimating gait parameters [19]. However, knowledge of the 3D forces and moments in the frontal and sagittal planes of the feet are required to estimate the CoM, XCoM and DSM towards objective evaluation of dynamic balance [12]. Studies have shown estimations of 3D forces/moments from 1D plantar pressure by using analytic and machine learning methods. Forner-Cardeno et al. [20] showed analytic derivation of 3D forces from 1D plantar pressure data, but his method relies on force plate data. Machine learning techniques such as linear regression modelling, and artificial neural networks have been shown to confidently predict 3D forces and moments from 1D plantar pressure [21–24]

In this study, linear regression modelling is used to predict 3D forces and moments from 1D plantar pressures. The knowledge is extended to estimate the CoM, XCoM and DSM. Overall, the objective of this study is to assess pressure insoles coupled with IMU as a lightweight and wearable alternative towards objective evaluation of gait and dynamic balance.

2. Materials and Methods

2.1. Measuring System

ForceShoes^{TM} contain two 3D force/moment sensors, and two IMUs on each foot as seen in Figure 1a. The data from the IMU located at the forefoot of each foot is used for analysis. The data from the 3D force/moment sensors and IMUs are sent to an Xbus that transmits data wirelessly to a PC. An ultrasound system is also placed on the ForceShoes^{TM}. The transmitter and receiver of the ultrasound system is placed on the right and left foot respectively. The transmitter and receiver are synchronized and the data is transmitted via Bluetooth to a PC. The pressure insole system (medilogic® insoles from T&T medilogic Medizintechnik GmbH, Schonefeld, Germany), consists of a thin insole with 151 resistive pressure sensors and is placed within the ForceShoes^{TM} and can be seen in Figure 1b. The insoles were held in place using tape to eliminate slippage. The wireless transmitters of the pressure insoles and ForceShoes^{TM} are worn as a belt around the waist. The 3D force/moment sensors, IMUs of the ForceShoes^{TM} and the pressure insoles were sampled at 50 Hz. An Extended Kalman Filter improves the estimation of the foot position, with inputs from the ultrasound system at an update frequency of 13 Hz [8].

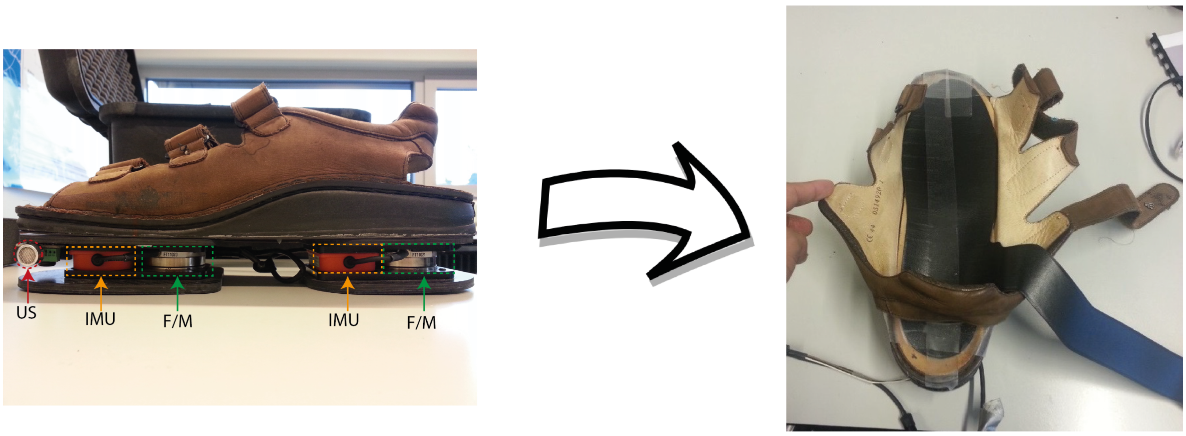

Figure 1. (**a**) Side view of right ForceShoe^{TM}. US represents the ultrasound transmitter, F/M denotes the 3D force/moment sensors. (**b**) Top down view of the ForceShoe^{TM} fitted with pressure insole.

2.2. Participants

Ten healthy subjects were recruited for the study. All subjects gave their informed consent before their participation. The study was conducted in accordance with the Declaration of Helsinki, and the protocol was approved by the Ethical Committee of the faculty. The inclusion criteria included subjects with no history of stroke, impaired gait or leg injury. Nine subjects were males and the size of the ForceShoes^{TM} used was 44 (European Size Chart). The average height, weight, age, and leg length of the subjects was 1.77 ± 0.05 m, 76 ± 6 kg, 25 ± 2 years, and 0.91 ± 0.3 m respectively. Leg length is the length of the leg measured from the hip joint to the ground [25].

2.3. Experimental Protocol

The ultrasound system on the ForceShoes^{TM} was calibrated using a calibration board. The calibration board calibrated the ultrasound distance measurement to the actual distance between the foot. The subjects were asked to perform the following tasks in order:

a *No Contact*
During this activity, the subject is asked to sit on a chair and raise both legs off the ground. The ForceShoes^{TM} are calibrated to 0 N force on both feet. After unloading, the subject repeats the task and a 10 second reading is obtained from the ForceShoes^{TM} and pressure insoles. This is the *'No Contact'* task.

b *10 Metre Walk - Normal*
During this activity, the subject is asked to walk for 10 metres over a straight line unobstructed path. The subject is first asked to stand still with the feet placed parallel. Once the researcher shouts 'Start', the subject starts walking along a straight line at his preferred *normal walking speed*. The time taken between start and stop of the walking is measured using a stopwatch. This activity is repeated six times. This is the *'10 Metre Walk - Normal'* task.

2.4. Objective Evaluation of Gait and Dynamic Balance

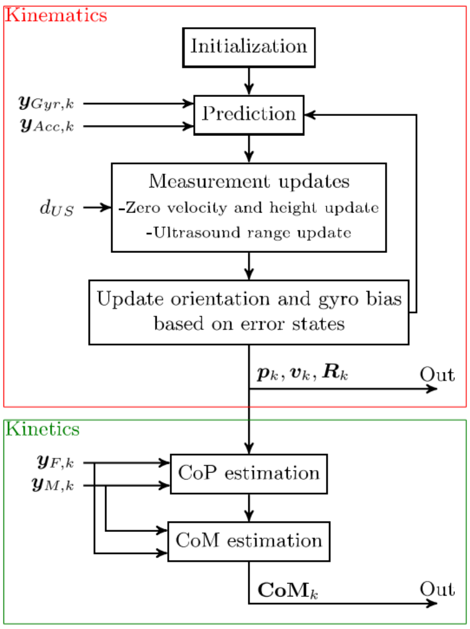

Figure 2. Kinematics and kinetics derived from the ForceShoes^{TM} using an Extended Kalman Filter. The states predicted by the Extended Kalman Filter are position, instantaneous velocity, orientation error and gyroscope bias error [10].

2.4.1. Gait

IMUs and ultrasound was used for estimating foot positions, from which gait parameters such as step length, and step width is obtained. Weenk et al., [8], validated this foot position estimate as a function of time. Position, instantaneous velocity, orientation error and gyroscope bias error are states predicted by an Extended Kalman Filter [8]. Error between predicted and measured data was used to correct the process and measurement noises for every measurement sample. Measurement updates include foot position and instantaneous velocity measured from the IMU, zero velocity instances, height of IMU during zero velocity and relative feet distance from ultrasound system. The process is presented in Figure 2. The output of the Extended Kalman Filter provides an accurate estimation of foot positions which is used to locate the Centre of Pressure (CoP).

2.4.2. Dynamic Balance

Estimation of CoM is the first step towards evaluating dynamic balance. Low and high frequency components of CoM were estimated using two separate algorithms and fused using a complementary filter, to improve estimation accuracy [12]. The first algorithm performs low pass filtering of the CoP to estimate the position of CoM, also referred to as Stage 1. The second method estimates CoM by double integration of the GRF based on Newton's second law, referred hereafter as Stage 2.

In Stage 1, the Centre of Pressure for each foot is estimated using the following algorithm.

$$\mathbf{x}_{CoP,foot} = \begin{pmatrix} \frac{-M_y}{F_z} \\ \\ \frac{M_x}{F_z} \\ \\ 0 \end{pmatrix} \tag{1}$$

In this study, the X axis is along the walking direction and Z axis is the vertical axis. The Y axis, found by Right Hand Rule, points left of the walking direction. All data is expressed in the global coordinate frame. In Equation 1, F_z is the vertical ground reaction force (GRF), and M_y and M_x denote the moments in the respective axes. The CoP trajectory over the walking trial was weighted with the relative magnitude of the GRF under each foot and is given as follows.

$$\mathbf{x}_{CoP} = \frac{\|\mathbf{F}_l\|}{\|\mathbf{F}_l + \mathbf{F}_r\|}\mathbf{x}_{CoP,l} + \frac{\|\mathbf{F}_r\|}{\|\mathbf{F}_l + \mathbf{F}_r\|}\mathbf{x}_{CoP,r} \tag{2}$$

Here, the $\mathbf{F}_l$ and $\mathbf{F}_r$ represent the total GRF in the left and right foot respectively. The $\mathbf{x}_{CoP}$ was then low pass filtered at 0.4 Hz to obtain the $\mathbf{x}_{CoM,S1}$. The cut off was optimal for the complementary filter, and for continuous walking.

In Stage 2, Newton's second law was used to estimate the acceleration of the body from the net force acting on it. The body mass m_{body} can be embodied at the CoM and the acceleration of the CoM is given as follows.

$$\mathbf{a}_{CoM} = \frac{\mathbf{F}_t}{m_{body}} + \mathbf{g} \tag{3}$$

Here, $\mathbf{F}_t$ is the net force acting on the body, and $\mathbf{g}$ is the gravitational acceleration. The CoM position was derived from double integrating the $\mathbf{a}_{CoM}$.

$$\mathbf{v}_{CoM} = \mathbf{v}_0 + \int_{t_0}^{t} \mathbf{a}_{CoM}(t)dt \tag{4}$$

$$\mathbf{x}_{CoM,int} = \mathbf{x}_0 + \int_{t_0}^{t} \mathbf{v}_{CoM}(t)dt \tag{5}$$

$$\mathbf{x}_{CoM,S2} = HighPassFilter(\mathbf{x}_{CoM,int}) \tag{6}$$

Here, $\mathbf{v}_0$ and $\mathbf{x}_0$ denote the initial velocity and position respectively. $\mathbf{x}_{CoM,S2}$ was obtained by applying a high pass filter to $\mathbf{x}_{CoM,int}$ with cut off at 0.4 Hz. This is the same cut off as that of Stage 1 low pass filter. The $\mathbf{x}_{CoM,S1}$ and $\mathbf{x}_{CoM,S2}$ were then fused to obtain the $\mathbf{x}_{CoM}$.

$$\mathbf{x}_{CoM} = fusion(\mathbf{x}_{CoM,S1}, \mathbf{x}_{CoM,S2}) \tag{7}$$

The projection of the extrapolated centre of mass, or XCoM′, as seen in the Figure 3 was obtained by the following equation.

$$XCoM' = CoM' + \frac{\mathbf{v}_{CoM}}{\omega_0} \tag{8}$$

Here CoM' is the vertical projection of the CoM on the ground, and $\mathbf{v}_{CoM}$ is the velocity of CoM and an indicator of the direction of movement. $\mathbf{v}_{CoM}$ is normalised to ω_0 which is given as $\sqrt{g/l_0}$, where g is the gravitational acceleration and l_0 is the vertical CoM position. The dynamic stability margin (DSM) is the shortest distance between the projected XCoM, i.e., XCoM′ and BoS [14]. In this study, the shortest distance is measured with respect to the frontline of BoS [10]. It is an indicator of the stability during continuous walking. If the DSM is positive i.e., if the XCoM′ is beyond the frontline of BoS, the person is dynamically unstable. The person would need to displace at least one foot to make the BoS larger, thereby stabilizing and preventing fall. If the DSM is negative i.e., the XCoM′ is within the BoS, the person is dynamically stable. In this case, extra foot displacement is not needed to stabilize from falling over.

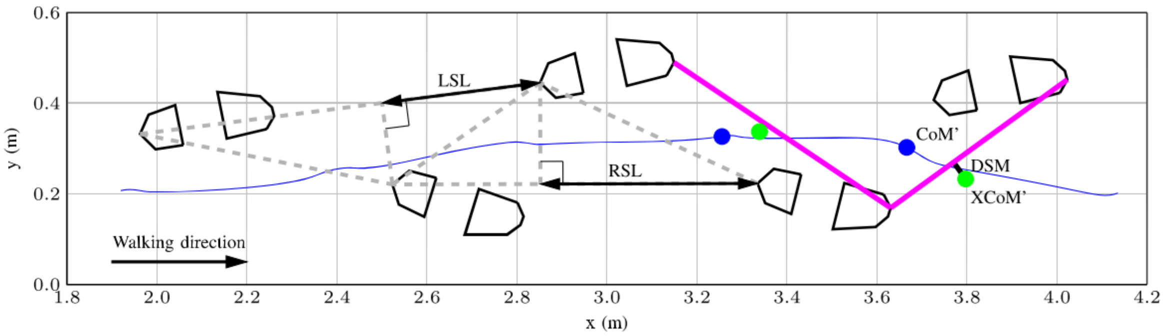

Figure 3. Foot positions during walking observed top-down. LSL and RSL stand for Left Step Length and Right Step Length respectively. The CoM′ and XCoM′ are the projections of the CoM and XCoM on the ground. The blue line depicts the trajectory of CoM′. The purple lines denote the frontline of the BoS. DSM is the shortest distance between the XCoM′ and the frontline of the BoS [10]

2.5. Estimation of 3D forces and moments from the Pressure Insoles

In order to implement Stages 1 and 2 we require information about the 3D forces and moments of the feet. This information can be derived from the ForceShoes$^{\text{TM}}$, and therefore the 2 stages can be completed to estimate $\mathbf{x}_{CoM}$, XCoM′, and DSM. As the pressure insoles are only able to provide the 1D plantar pressures under the feet, a linear regression model was created to predict the 3D forces and moments from 1D plantar pressure data.

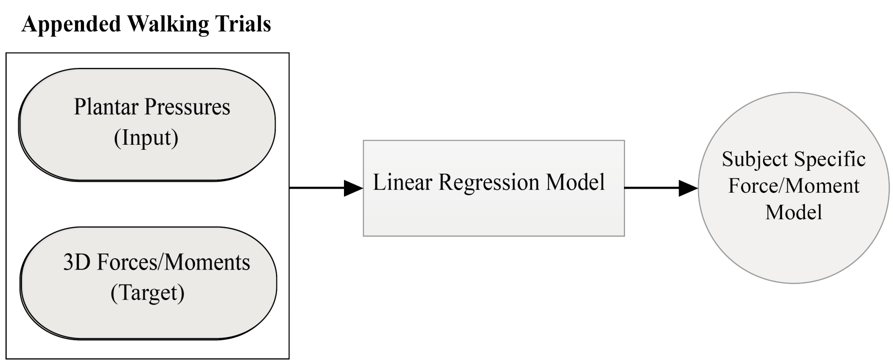

Figure 4. All walking trials per subject is appended to obtain a subject specific model.

First, the data between the ForceShoes^{TM} and pressure insoles were synchronized using cross correlation. Two seconds were snipped at the beginning and at the end of each walking trial. This is followed by appending all walking trials for each subject as shown in Figure 4. A linear regression model was fitted using MATLAB^{TM} command $f$itlm. The input to the model was the plantar pressures from the 151 sensors of the pressure insole and the targets were the 3D forces and moments from the ForceShoes^{TM}. This model is subject specific and estimates 3D forces and moments, given the plantar pressure information for each foot during a walking trial, as seen in Figure 5. For further details on a representative linear regression model used in this study, refer Appendix C. The model can also predict 3D forces and moments during quiet standing, initiation of walking, cyclical walking and deceleration of walking and stopping. The modelling process was repeated to create linear regression models for every subject.

Using the subject specific model, the 3D forces and moments were estimated for each walking trial and subsequently, $\mathbf{x}_{CoM}$, XCoM′, and DSM are calculated. The results were then compared with the results from the ForceShoes^{TM}.

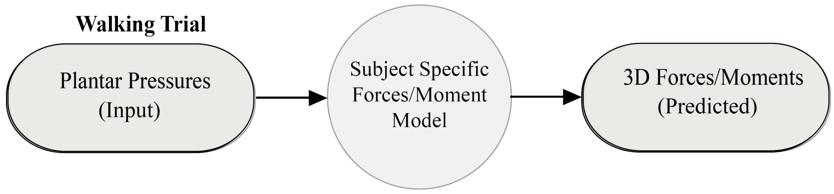

Figure 5. The subject specific model is used to predict the 3D forces and moments for each walking trial.

2.6. Statistical Analysis

To test the linearity between results obtained from the measured ForceShoes^{TM} data and the predicted data from subject specific model, Pearson's Correlation was calculated. The root mean square (RMS) of the differences between the data was studied to understand the agreement between them.

2.7. Classification of Stability

The DSM, an indication of dynamic balance, denotes the stability during walking. It would be useful to compare if the subject specific model can classify rightly if the XCoM′ was beyond or within the frontline of the BoS. If the XCoM′ was beyond the frontline of BoS, this can be called as an unstable sample point. This would require an extra step to stabilize from falling over. The sample point is stable if the XCoM′ was within the BoS. A confusion matrix is created to see how the DSM estimation by the predicted and measured values agree.

3. Results

3.1. Experimental Results

Speed of walking affects the periodicity of steps taken. This has an influence on the predictive capability of the linear regression model. Therefore, the walking trials were evaluated for outliers. This was done by plotting a boxplot of the average peak walking speed of each subject for each trial. The average peak walking speed was calculated by averaging the peak velocity of the feet during walking. The peak velocity is the maximum instantaneous velocity of the foot during a single step. The boxplot for the trials during the *'10 Metre Walk - Normal'* task is seen in Figure 6. The outliers, denoted by '+' consist of trials where the subject was either too slow or too fast compared to their other trials. Outliers were seen for Subjects 2, 5 and 7 and these trials were removed from analysis. Some trials suffered from sensor issues and missing samples in the data transmission. These trials were also removed from analysis. It was made sure that each subject had at least four valid walking trials. The average walking speed of the selected trials is shown in Table 1.

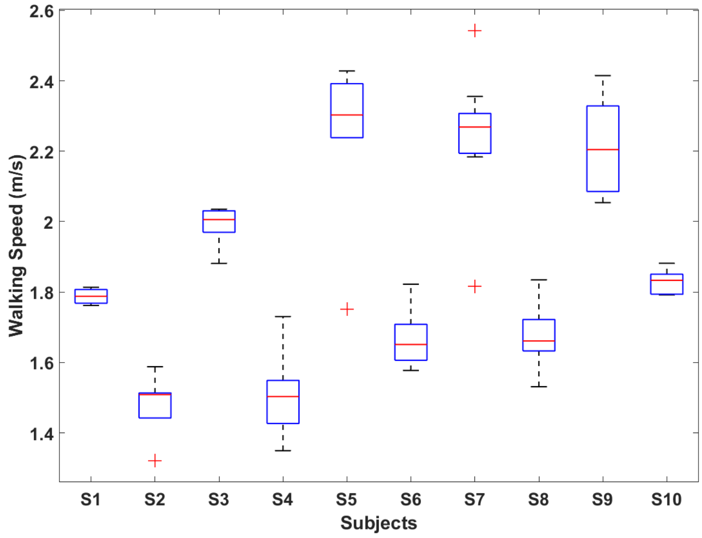

Figure 6. Boxplot visualisation of distribution of average peak walking speed for each subject during the *'10 Metre Walk - Normal'* task. The peak instantaneous foot velocity was calculated for each step. This was averaged over the walking trial to obtain the average walking speed. The outliers indicated by '+' were removed from analysis.

Table 1. List of average peak walking speeds for the '10 Metre Walk - Normal' task. The average peak speed among all subjects is 1.88 ± 0.32m/s.

Subject	**Walking Speed** (m/s)
Subject 1	1.79 ± 0.02
Subject 2	1.51 ± 0.05
Subject 3	1.99 ± 0.05
Subject 4	1.51 ± 0.12
Subject 5	2.33 ± 0.07
Subject 6	1.65 ± 0.08
Subject 7	2.27 ± 0.05
Subject 8	1.66 ± 0.07
Subject 9	2.22 ± 0.15
Subject 10	1.83 ± 0.03

The selected trials were subsequently used for analysis. IMUs and ultrasound system are the sources for foot position estimation. Therefore, temporal gait parameters were not compared between ForceShoes^{TM} and pressure insole systems. Dynamic balance measures were estimated and compared for the valid trials. The trials for each subject were appended for the subject specific linear regression model. This model was then used to predict the 3D forces and moments for each walking trial.

3.2. Representative Study

A typical example picked at random is described here. The data used is from the first walking trial of Subject 9. The Figure 7 shows the prediction of 3D forces and moments from 1D plantar pressure information using the subject specific model for the left leg. These forces and moments were compared with the measured forces and moments from the ForceShoes^{TM}. The predicted information was then used to estimate CoM as seen in Figure 8 and subsequently used to estimate the XCoM and DSM. These parameters were also compared with the estimations by the ForceShoes^{TM}.

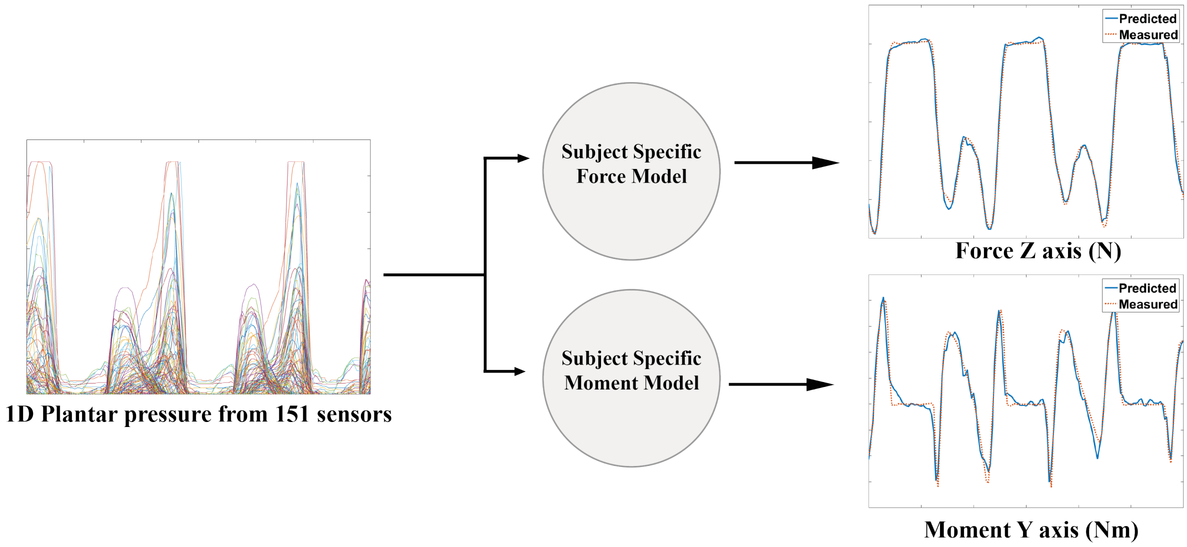

Figure 7. 1D plantar pressure from 151 sensors on the left leg, for the first walking trial is fed into the subject 9 force/moment model to obtain the 3D forces/moments. One axis of each, the forces and moments are shown here for representation. The solid blue line shows the predicted force/moment. The dashed red line is the measured force/moment from the ForceShoes^{TM}.

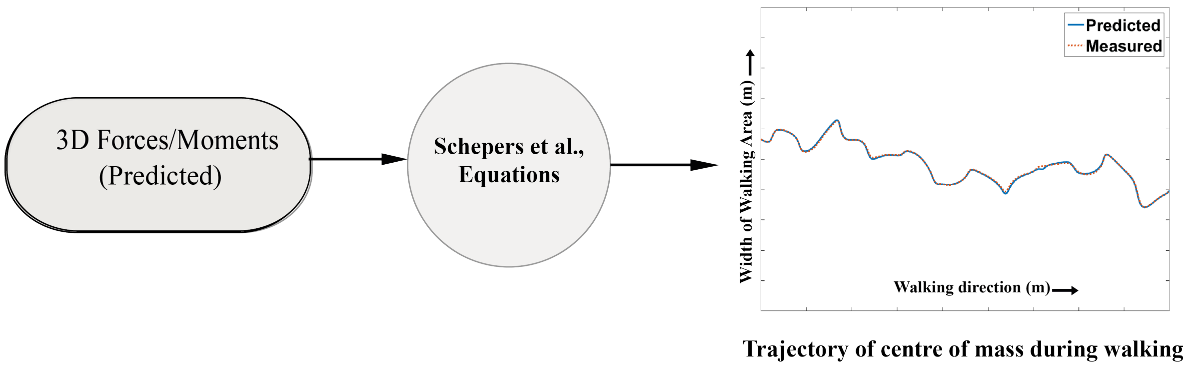

Figure 8. The 3D forces/moments predicted for each walking trial is processed using Schepers et al., [12] to obtain the center of mass trajectory over the walking trial. The CoM trajectory is shown as a solid blue line. The dashed red line is the CoM estimated from measured forces and moments from the ForceShoes^{TM}.

3.3. Comparison between predicted and measured data

The data was processed for all subjects for all valid walking trials. The predicted model output and measured 3D forces and moments from the ForceShoes^{TM} were compared. Pearson's correlation was calculated and shown in Figure 9. The figure shows the percentage of correlation for each axis along with error bars which denote the standard deviation.

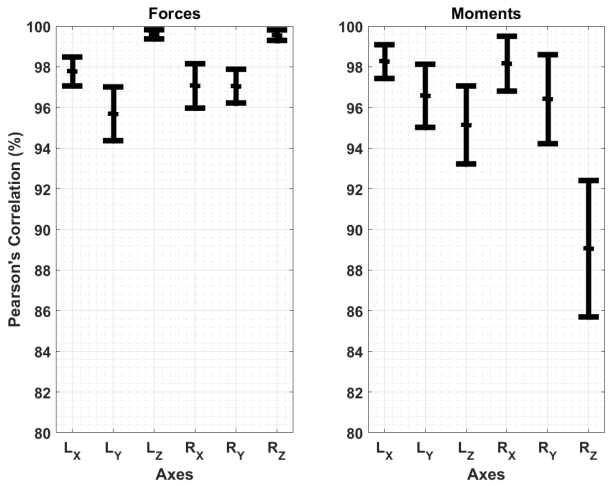

Figure 9. Average Pearson's correlation along with standard deviation between the predicted and measured 3D (**a**) forces and (**b**) moments for each axis. For instance, L_X denotes the X axis of the Left leg.

RMS of the differences of the predicted and the measured 3D forces and moments was calculated and normalized to the range of the measured value. The average relative RMS of the differences for each axis along with standard deviation is plotted in Figure 10.

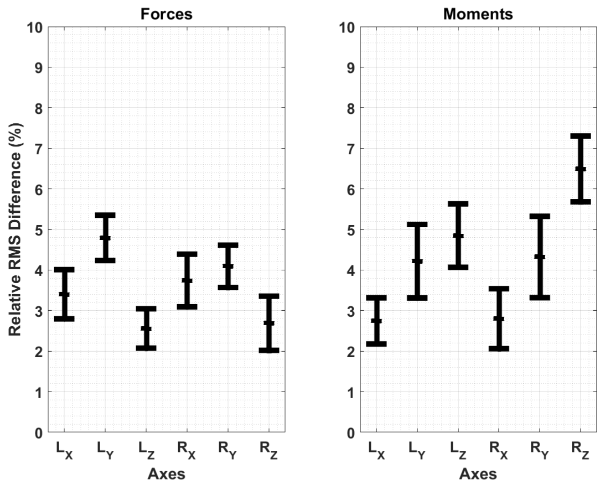

Figure 10. Average relative RMS of the differences along with standard deviation between the predicted and measured 3D (**a**) forces and (**b**) moments for each axis. For instance, L_X denotes the X axis of the Left leg. The RMS of the differences is normalised to the range of measured value.

The predicted and measured 3D forces and moments were further processed to obtain the position of centre of mass in the two stages, $\mathbf{x}_{CoM,S1}$ and $\mathbf{x}_{CoM,S2}$, derived from the Equations 2 and 6. The RMS of the differences between the values from the predicted and measured data for each walking trial is calculated and normalised to the range of the measured values. This is shown in Figures 11 and 12.

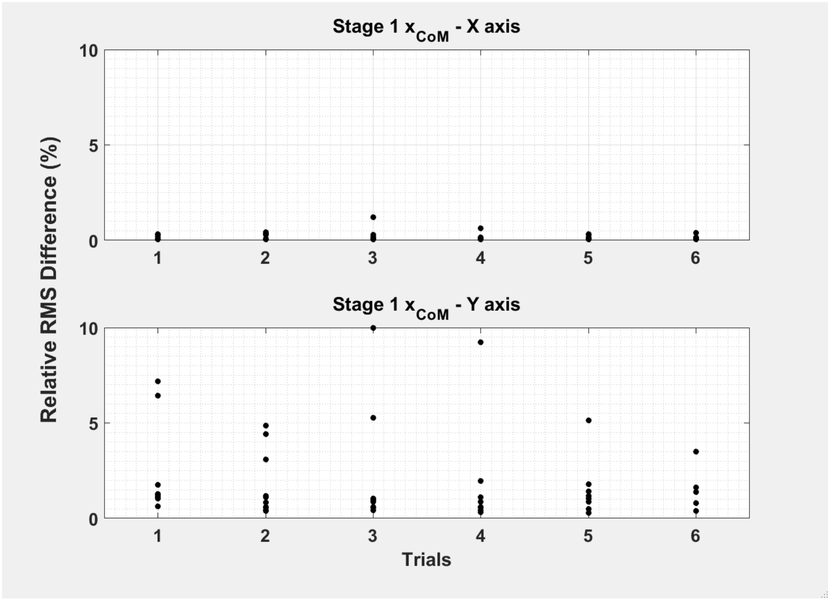

Figure 11. RMS of the differences normalised to the range of measured data. This is between Stage 1 $\mathbf{x}_{CoM,S1}$ from predicted and measured 3D forces/moments in (**a**) X and (**b**) Y axis. Each dot represents the relative RMS of difference for one walking trial for a subject. The graph is a cluster plot of all walking trials of all subjects.

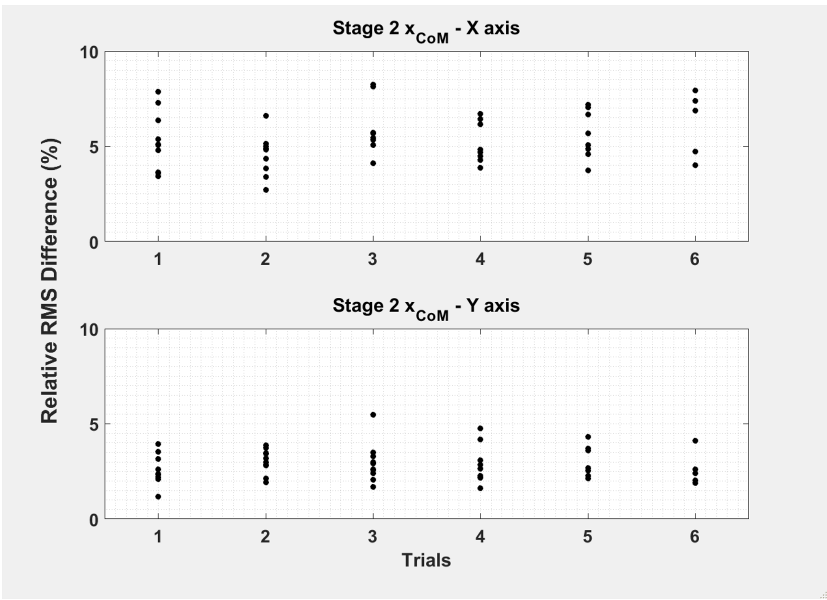

Figure 12. RMS of the differences, normalised to the range of measured data. This is between Stage 2 $\mathbf{x}_{CoM,S2}$ from predicted and measured 3D forces/moments in (**a**) X and (**b**) Y axis. Each dot represents the relative RMS of difference for one walking trial for a subject. The graph is a cluster plot of all walking trials of all subjects.

The two stages were fused to improve the accuracy of estimation of $\mathbf{x}_{CoM}$. The fused x_{CoM} was compared and presented in Appendix D.1, following which the XCoM was estimated, according to Equation 8. The results from the predicted and measured data was compared. Figure 13 and 14 show the comparison performed in the X and Y axis respectively.

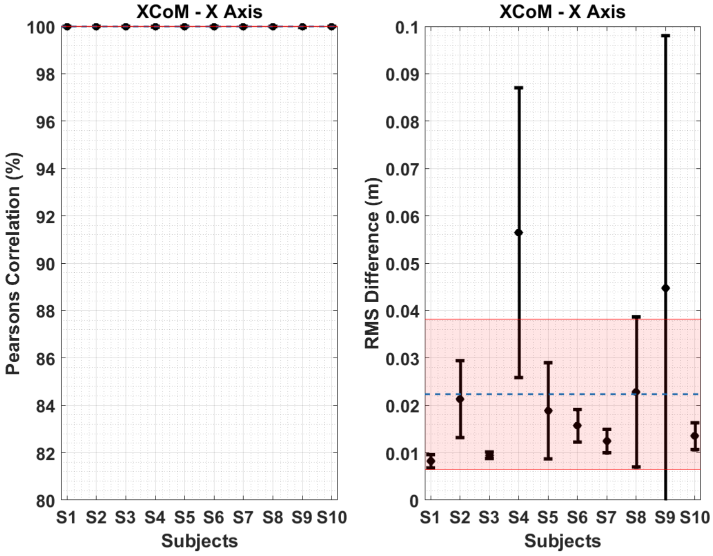

Figure 13. (**a**) Pearson's Correlation and (**b**) RMS of the differences between the XCoM estimated from predicted and measured 3D forces/moments in the X axis. The mean of the values for each subject is depicted as filled circles with an error bar that denotes its standard deviation. The horizontal blue dashed line shows the mean value of the measurements among all subjects. The light red region denotes the standard deviation from the mean.

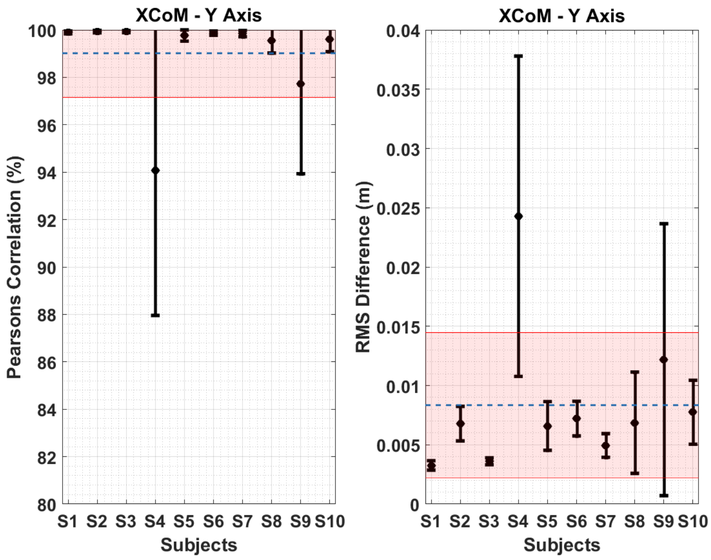

Figure 14. (**a**) Pearson's Correlation and (**b**) RMS of the differences between the XCoM estimated from predicted and measured 3D forces/moments in the Y axis. The mean of the values for each subject is depicted as filled circles with an error bar that denotes its standard deviation. The horizontal blue dashed line shows the mean value of the measurements among all subjects. The light red region denotes the standard deviation from the mean.

In Figures 13 and 14, the horizontal blue dashed line shows the mean value of the measurements among all subjects in each graph. The light red area denotes the standard deviation of the mean value. The average over all walking trials for each subject is depicted as filled circles with an error bar that denotes the standard deviation.

The DSM is then calculated, compared and displayed in Figure 15.

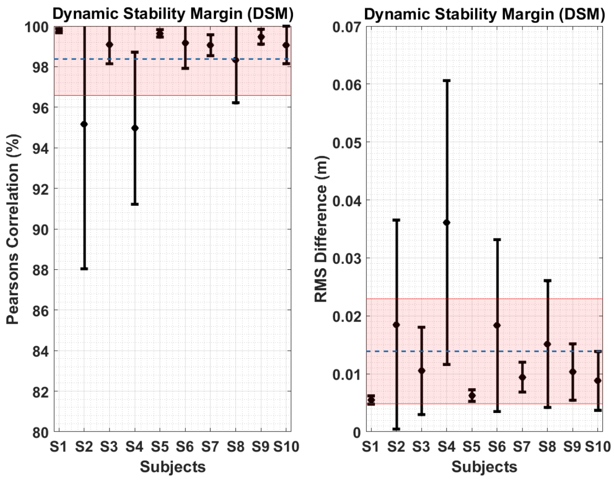

Figure 15. (**a**) Pearson's Correlation and (**b**) RMS of the differences between the estimated DSM from predicted and measured 3D forces/moments. The mean of the values for each subject is depicted as filled circles with an error bar that denotes its standard deviation. The horizontal blue dashed line shows the mean value of the measurements among all subjects. The light red region denotes the standard deviation from the mean.

3.4. Classification of Stability

During the population of the confusion matrix, the actual class refers to the stability according to DSM from the measurement by the ForceShoes^{TM} and the predicted values are derived from the subject specific model. The sample points from all walking trials from all subjects in the *'10 Metre Walk - Normal'* task was classified as stable or unstable and compared as seen in Table 2.

Table 2. Confusion Matrix showing classification of sample points from walking trials as dynamically stable or unstable

		Predicted		
		Stable	Unstable	Total
Actual	Stable	14797	140	14937
	Unstable	139	2831	2970
	Total	14936	2971	17907

Derivatives are obtained from the confusion matrix and displayed in Appendix E. The sensitivity, specificity and accuracy are shown below.

$$\begin{aligned} Sensitivity &= \frac{\text{Unstable points predicted rightly}}{\text{All actual unstable points}} = 95.3\% \\ Specificity &= \frac{\text{Stable points predicted rightly}}{\text{All actual stable points}} = 99.1\% \\ Accuracy &= \frac{\text{Rightly predicted points}}{\text{All Points}} = 98.4\% \end{aligned} \tag{9}$$

3.5. Addressing the different sections of Walking trials

The results so far has been shown for the entire walking trial. This includes a quiet standing phase, an initial step, a continuous walking pattern followed by a deceleration step before the foot comes to a complete halt. While creating a linear regression model, most of the walking data is cyclical and repetitive. Therefore, the walking trial was split into sections as seen in Figure 16 and the performance of the method for each section is studied. Section 1 denotes the quiet standing and initial step taken by the respective foot. Section 2 denotes cyclical walking and section 3 is the decelerating step including the halting of the walking trial. The average RMS of the estimations of CoM, XCoM and DSM for different sections are displayed in Table 3. Note that the subject specific model for the entire walking trial was applied to each section.

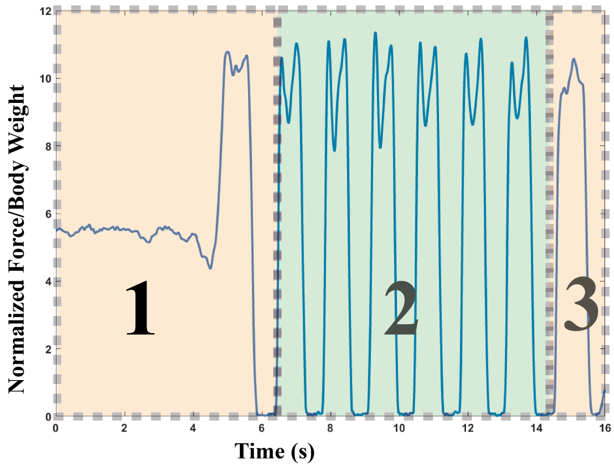

Figure 16. A representative walking trial denoted by changes in the magnitude of force in the left foot of subject 6. This is the lagging foot, or in other words, the right foot takes the first step. During the analysis in the previous sections, the entire walking trial is considered. Here, the walking trial is split into three sections and the performance in each section is compared. Section 1 is the quiet standing phase along with the first step on this foot. Section 2 is the duration of cyclical walking. Section 3 is the last step before which the subject stops walking.

Table 3. Section wise comparison of the RMS of the differences and the classification accuracy. The data is split as seen in Figure 16 and each section is analysed individually. The values shown here are the average over all walking trials of all subjects. The standard deviation is within brackets.

	CoM X axis (m)	**CoM Y axis** (m)	**XCoM X axis** (m)	**XCoM Y axis** (m)	**DSM** (m)	**Accuracy** (%)
Entire Trial	0.008 (0.005)	0.004 (0.002)	0.022 (0.016)	0.008 (0.006)	0.014 (0.01)	98.5
Section 1 and 3	0.005 (0.002)	0.003 (0.001)	0.011 (0.007)	0.005 (0.003)	0.011 (0.006)	99
Section 2	0.01 (0.007)	0.004 (0.002)	0.029 (0.02)	0.010 (0.008)	0.019 (0.014)	94.5

4. Discussion

The objective of the research was to evaluate pressure insoles and IMUs as an alternative to the ForceShoes^{TM}. This discussion is structured in order of the results presented. The 3D forces/moments predicted from the subject specific model and measured from the ForceShoes^{TM} were compared to address the performance of the model. First, the correlation was studied using Pearson's Correlation as seen in Figure 9. The figure shows high correlation between the predicted and measured values for both the 3D forces and moments. It is observed that the correlation is higher for the Z axis of the forces as compared to the X and Y. The Z axis corresponds to the vertical force during the walking trial and it is known that the 1D plantar pressures capture the vertical forces better than shear forces

[18]. Similarly, higher correlation in the Z axis was shown in other studies [22–24]. In Figure 9b, it is observed that the correlation is lower in the Z axis as compared to the X and Y, for the moments. Moment is a cross product of distance and force as shown in Equation 10, where moment in the Z axis is a function of the forces in the X and Y axes. As these forces have lower correlation than the force in Z axis, it follows that the moment in the Z axis has lower correlation than the rest. However, one must note that in this study only the moments in the X and Y axis are necessary for estimation of CoM as seen in Equation 1.

$$\mathbf{M} = \mathbf{r} \times \mathbf{F} = \begin{vmatrix} i & j & k \\ r_X & r_Y & r_Z \\ F_X & F_Y & F_Z \end{vmatrix} \tag{10}$$

Similar trends were shown in Sim et al., [24]: the forces in the Z axis had the highest correlation followed by the X axis. Also, in case of moments, Z axis showed the least correlation. Comparatively, except for forces in X axis, the current study shows slightly higher correlation in terms of forces and moments in all three axes than that described in Sim et al. [24]. The comparison can be seen in Table 4. The values displayed for the current study are the correlations averaged between the right and left foot. A major difference between this study and that of Sim et al., is that Sim et al., used three different walking speeds - fast, normal, and slow for training a wavelet neural network.

Table 4. Comparing the correlation found in the current study and Sim et al. [24]

Measurement	Current Study (%)	Sim et al. (%)
Force X	97.4	97.6
Force Y	96.4	85.3
Force Z	99.6	98.8
Moment X	98.2	87
Moment Y	96.5	88.1
Moment Z	92.1	84.7

Given a high correlation in the 3D forces/moments, it would be interesting to see how the differences are, to throw light on the accuracy of the model. The RMS of the differences in Figure 10 can be used for this purpose. The figure depicts the percentage error normalised to the range of the measured values. In Figure 10a, we observe that the percentage of mean error is lower for the force in Z axis and higher for the Z axis in terms of moments on both feet. This follows the reasoning discussed for the correlations earlier. Mean error is highest for the Y axis for the forces on both feet. A possible explanation could be the arrangement of sensors in the insole. The forces in the Y axis are measured across fewer sensors as compared to the number of sensors placed in the X axis, which is along the length of the foot.

Once the 3D forces and moments are analysed, their contribution to the estimation of CoM has to be ascertained. The accuracy of estimation of CoM also depends on the relative foot positions. This is estimated using IMUs and ultrasound, and remains the same for both ForceShoes$^{\text{TM}}$ and pressure insole. Therefore, it is not compared here.

Following this, the two Stages were performed to calculate the position of the CoM. From Equation 1, we see that the vertical force and moments in the X and Y axis are necessary for the estimation of CoP. This was used to obtain Stage 1 position of CoM. Figure 11 shows the differences for position of CoM in Stage 1 for the X and Y axis normalised to the range of the measured values. The figure displays the differences for every walking trial (maximum of six trials per subject), and clusters data from all subjects. The vertical or Z axis is ignored for further analysis as we are interested in the projections on the ground. Figure 11a shows that most of the trials have a relative RMS of differences less than 5 %. The errors are higher for the Y axis in Figure 11b. The absolute values of the RMS of the differences are shown in Appendix D.2, in Figure D.3.

Shear forces contribute to the high frequency components of the CoM in Stage 2. The accuracy of CoM estimation without the contributions of the shear forces should be considered for future study.

Here, we observe from Figure 12a, that the error margins for the X axis are higher than that of Stage 1 as shown in Figure 11a. However, the range of errors for the Y axis in Figure 12b is smaller than that seen for Stage 1 in 11b. The graphs show that there is higher error in the high frequency component of the position of CoM in the X axis. The absolute values of the RMS of the differences is shown in Appendix D.2, in Figure D.4.

Next, the data from the two stages was fused. The fused x_{CoM} was compared and presented in Appendix D.1, following which the XCoM was estimated. Figure 13 shows the Pearson's Correlation and RMS of the differences. Figure 13a shows that the average correlation in the X axis is high for all subjects. The mean of the RMS of the differences for all subjects is 2.2 cm. The farthest deviation from the mean is seen in subject 4, who has a mean close to 5.6 cm. The subjects 4 and 9 show large standard deviation compared to the other subjects and this can be related to a large deviation in their average peak walking speed as seen in Table 1. The comparison for the Y axis is shown in Figure 14. The mean inter-subject correlation in Figure 14a is 99 %. The RMS of differences in the Y axis is lower than the X axis and can be seen in Figure 14b, where the mean of all subjects is 0.85 cm and the farthest mean is for subject 4 at 2.4 cm. Subjects 4 and 9 show large deviations in both the correlation score and RMS of differences among trials.

Despite considering the largest RMS of differences, the comparisons show good confidence in the method described. High correlation between the 3D forces and moments and the subsequent estimations show that a subject specific linear regression model is viable in replacing the function of ForceShoes^{TM} by the pressure insoles. Stroke survivors could be asked to wear the pressure insoles and perform a few walking trials to calibrate a subject specific model. This model can be stored in the on board memory to be used for later prediction of gait parameters. This can help model the gait variability seen between stroke subjects [3], which may be predicted less accurately if a generalized model is used for all subjects.

Next, the differences in the DSM is analysed in Figure 15. The average correlation is 98.5% and the mean RMS of differences is 1.4 cm. However, subjects show large deviations from their means in both correlation and mean RMS of differences. The confusion matrix to compare the classification of stable and unstable sample points by the predicted and measured values is shown in Table 2. The sensitivity of the model in classifying unstable sample points rightly is 95.3 %. This relates to a 95.3 % confidence of rightly classifying subjects if they are beyond the frontline of BoS. However, the specificity of the model in classifying points as stable or within the BoS is higher at 99.1 %. The higher specificity is due to a larger set of sample points for the stable class. This includes quiet standing duration, where absence of any movement leads to better classification. The accuracy of the model, defined as the ability to rightly classify all points is 98.4 %. The high values of specificity, sensitivity and accuracy show that the DSM estimated from the predicted 3D forces/moments is highly reliable.

Table 3 shows the comparison between different sections of the walking trial. It is seen that the estimations of CoM, XCoM and DSM is better for the combined sections 1 and 3. Most variability in the estimation is seen for section 2. The RMS of the differences in section 2 is higher for estimations of CoM, XCoM and DSM as compared to the entire walking trial.

Pressure insoles are prone to slippage if it is not fastened to the sole of the shoe. Although tape was used to hold it in place, there are possibilities of curving of the insole during walking. The layer of sock between the feet and insole reduces the friction between them aggravating the problem. This slippage must be considered to avoid introduction of creep plantar pressure readings from the sensors. This may lead to errors in the prediction by linear regression model.

Given its shortcomings, the subject specificity of the predictive model has advantages over existing studies [21–24]. It has higher accuracy of predicting 3D forces and moments and maps quiet standing, and variable walking. Although they form an integral part of activities of daily life, these conditions were not considered in earlier studies. Another aspect of this approach is its modularity. Instead of validating a new approach towards estimation of CoM, the current method pre-processes the input information such that it can be used in an existing approach, namely the Schepers et al. approach [12]. As the Schepers et al. approach has been validated against standard systems, any additional errors in the current method would mostly originate from the input applied to the approach.

Therefore, a subject specific model to predict forces/moments can be confidently used to implement pressure insoles as an alternative wearable system.

4.1. Limitations

Each subject must walk a few times to obtain data for building the subject specific model. This would require a calibration phase where the stroke survivors should walk in order to create a subject specific model. Though this may increase the activity load on the survivor, it leads to a model that can better estimate the CoM. A hybrid method can also be considered as in the case of the Myo^{TM} armband (ThalmicLabs^{TM}, Canada). The armband can classify gestures based on the EMG input from 8 sensors across the arm. It contains a generic model built on a huge user database for this purpose. However, before any new user can use it, a calibration is performed that improves its predictive nature. A similar approach could be considered for a wearable that quantifies gait and balance for stroke survivors.

The current model depends on the speed of walking. Preliminary analysis showed that the model trained for an average walking speed fails to estimate 3D forces/moments for trials where the subject had a different walking speed. Therefore, a speed generalized model should be built. In this study a linear regression was used for creating the predictive model. This may lead to over or under fitting resulting in stray data points. Studies have shown that using neural networks, better accuracy in predicting 3D forces/moments can be obtained [21–23].

The walking trials involved in the study are straight line walking without much variation in the medio-lateral direction. Components such as turning can introduce shear forces directed towards the direction of turning. Variable walking during activities of daily life is highly different from a constrained lab walking trial. The accuracy of the model in incorporating these effects of variable walking should be studied in further trials.

Though the recruitment was not selective to sole size or in terms of gender, the participating group is not very diverse. There is only one shoe size tested with and only one female subject involved in the study. However, this would not have any effect on the current results or validity of the method.

Although the goal is to design a wearable system for stroke survivors, the study was performed on healthy subjects. Stroke survivors have different walking patterns which may vary within subjects based on the degree of impairment. Elements of behavioural substitution have not been implemented. Some subjects also use a walking cane for balance. The XCoM and DSM must be redefined in these situations and the regression model must be tested for its reliability.

Pressure insoles used in this study have many sensors per foot. Though this increases the accuracy of the model generated, inclusion of many sensors result in more calculations and increased power usage. Studies have shown that the number of sensors can be reduced and its location be optimised [22]. The effect of a reduced sensor set such as the use of an IEE® (IEE®, Luxembourg) insole, on the error margins and accuracy of stability estimation must be studied.

The medilogic® insoles cannot measure pressure values larger than $64N/cm^2$. There may be some instances of heel strike where the measured pressure may exceed this value. These values are lost due to the limitations of the measurement system. Another interesting question is if the change in insole shape influences the subject specific models created. Finally, the pressure sensors are resistive and may have sensor issues when there is a large change in temperature and heavy sweating.

4.2. Future Work

As mentioned earlier, this study doesn't include variability in walking speed. Therefore, a subject specific model that can predict estimate CoM over different walking speeds and daily life variable walking should be built. In the current system, 151 sensors are used in each foot to measure the plantar pressure. High sensor density offers higher accuracy but also results in higher costs and needs more processing power. Therefore, impact of reduction of sensors, such as use of an IEE® insole system must be studied. Another question is to study the accuracy of estimation of CoM, XCoM and DSM, while using only the IMUs and ultrasound distance sensing system. Another interesting objective is studying the contribution of shear forces towards the estimation of CoM.

5. Conclusions

Pressure insoles can be a lightweight and an inconspicuous alternative to ambulatory estimation of gait and balance. The study proves this by showing in stages, the correlation and RMS of the differences in the steps towards gait and balance measures. Once a wearable system is designed for patient use, the stroke survivor can perform an initial calibration, monitored by a clinician. Initial calibration can be done over an instrumented treadmill, using force plates, or using ForceShoes™, for instances of variable walking. Once calibrated, the stroke survivor can use this system in her/his activities of daily life. This will improve the monitoring of the improvement in mobility after stroke. This study is a positive step in the design of such a wearable for stroke survivors.

Acknowledgments: This project is funded by STW and is a part of project 7 under the Dutch National project NeuroCIMT. The medilogic® insoles were borrowed from Roessingh Research and Development, Enschede, The Netherlands. The experiments were conducted at the Biomedical Signals and Systems department, University of Twente, Enschede, The Netherlands.

Conflicts of Interest: The authors declare no conflict of interest. The founding sponsors had no role in the design of the study; in the collection, analyses, or interpretation of data; in the writing of the manuscript, and in the decision to publish the results.

Abbreviations

The following abbreviations are used in this manuscript:

IMU	Inertial Measurement Units
GRF	Ground Reaction Forces
CoM	Centre of Mass
CoP	Centre of Pressure
BoS	Base of Support
XCoM	Extrapolated Centre of Mass
DSM	Dynamic Stability Margin
RMS	Root Mean Square

Appendix A. Stroke

Cardiovascular diseases (CVDs) are the leading cause of death in the world [26] and account for 31.2 % of all global deaths. Six out of the nine targets in the global agenda on prevention and control of noncommunicable diseases determined by the World Health Organisation aims at reducing the incidence of CVDs [27].

Stroke is a CVD, and is caused when a blood vessel in the brain ruptures, or if there are blood clots present preventing normal flow [28,29]. Brain cells deprived from blood, and subsequently oxygen, die and abilities controlled by the dead region are lost. This include muscle control and memory. The Netherlands is home to close to 17 million people of which stroke accounts for 8.4% of annual deaths [30].

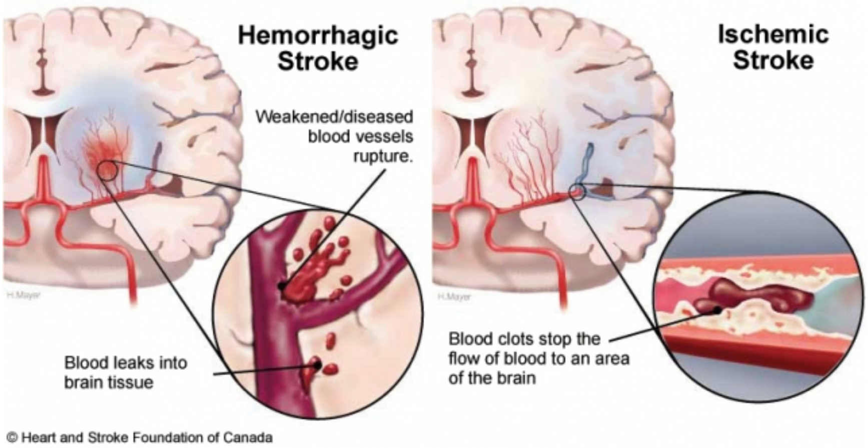

Figure A.1. Two causes of stroke are shown here. (**a**) shows the occurence of a Hemorrhagic stroke where there is leaking of a blood vessel. (**b**) shows Ischemic stroke caused by the presence of a blood clot [31]

The two kinds of stroke include haemorrhagic stroke and ischemic stroke. The former is the burst of a brain aneurysm or rupture of a blood vessel. Ischemic stroke occurs due to the presence of a blood clot. The two types are shown in Figure A.1. The incidence of ischemic stroke is higher than haemorrhagic stroke. Stroke survivors, unfortunately, cannot be recovered to their pre-stroke state of well being. This is because a segment of the brain is missing and complete recovery of the function of the missing region is impossible.

It is observed that women on an average live longer than men after stroke [31]. Common post stroke disabilities can be seen in physical, emotion and cognitive abilities [32]. Physical disabilities are manifested in the form of paralysis, hemiparesis, spasticity, drop foot, dysphagia, fatigue, incontinence, pain, seizures, sleep, and troubles with vision. Emotional disabilities include instances of depression, and events of pseudobulbar affects. Stroke survivors may also suffer from aphasia, memory loss, and vascular dementia which are cases of cognitive disabilities.

Hemiparesis, a result of stroke, affects the mobility of the stroke survivor. It is defined as weakness on one side of the body, contralateral to the hemisphere of the brain impacted by stroke [32]. Hemiparesis is observed in 80% of stroke survivors. Rehabilitation in the clinic following stroke has a major focus on training the subject to regain motor functions lost or weakened due to hemiparesis. This includes training to improve balance, walking, and improving ability to grasp objects and precision control of the arms and fingers. This helps improve strength and regain a part of the lost control on the affected side.

Pollock et al., [33] lists the treatment strategies and its efficacy for the upper limb alone. This includes bilateral arm training, biofeedback, bobath therapy, brain stimulation, constraint induced movement, electrical stimulation, mirror therapy, music therapy, repetitive task therapy, mental practice, robotic therapy, and task specific therapy. Among these, he finds that mirror therapy, constraint induced movement therapy, mental practice, virtual reality, and sensory interventions show positive evidences of benefits.

Dobkin et al. [6] describes the treatment strategies for the different disabilities caused due to stroke. In this review, Dobkin et al., suggests that slow walking helps improve speed and endurance in patients with hemiparesis. They also suggest repetitive tasks show positive impact on improving strength and balance.

Several clinical assessments have been devised to assess the activities of daily life, balance, and mobility of a subject after stroke [34]. This includes 10 Meter Walk Test, Berg Balance Scale, Dynamic Gait Index, Fugl-Meyer Assessment of Motor Recovery after Stroke, and Timed Up and Go among many others. These tests are monitored periodically to assess the improvement in using the treatment strategies.

There have been quite some National and European Union interests on addressing the problems associated with incidence of stroke. The NeuroCIMT project funded by the STW also has a major focus on understanding stroke and improving rehabilitation post stroke.

Appendix B. Pressure Insoles

Pressure insoles have been widely used for quantifying gait [17]. Several studies have validated them against standard force sensing systems such as force plates and instrumented treadmills [35–38]. Studies have also used pressure insoles for activity classification [39].

There are several insole systems available commercially as well as in research. A few commercial examples include IEE® (IEE®, Luxembourg), Orpyx® (Orpyx Medical Technologies, Canada), F-scan® (Tekscan, USA), medilogic®, Moticon® (Moticon®, Germany), footlogger® (3L Labs, South Korea), Sensoria® (Sensoria® Inc., USA), Pedar® (Novel, Germany), and Stridalyzer® (Retisense, India) among others. Pressure insoles can be characterized by their sensor design. Capacitive based pressure insoles consists of capacitive sensors. Two electrically charged conductors separated by a dielectric display a change in output voltage proportional to the applied pressure. Commercially available systems based on this type are the Moticon® insole (Moticon®, Germany) [35] and Pedar® insole (Novel, Germany). Resistive sensors are the commonly used sensors for pressure insoles. Pressure on the insole surface changes the resistivity of the sensor proportionally. Commercially available sensors include F-Scan® insole (Tekscan, USA), and medilogic® insoles which are used in this study. Another sensor type used in research is the implementation of hydrocells for pressure estimation. These sensors employ piezoresistive sensors within a fluid filled cell [40].

Other sensor types include piezoelectric, and piezoresistive based sensors. New sensor types have also been developed for measuring plantar pressure. This includes PSCR and opto-electronic systems. The PSCR is an elastomer sheet that has high resistive in its normal state. Once the sheet is pressed, the resistance varies according to the pressure applied. This can be read out and mapped to the pressure output. The sheet is patented by Nitta Industries Corporation [41]. Saito et al. [42], made use of this system in an insole to capture the plantar pressure during walking trials. The device construction can be seen in Figure B.1.

Another novel sensor system used for detecting pressure is optoelectronic sensors used by Crea et al [43]. In this system, an LED is present that emits light detected by a sensor placed in an adjacent compartment. The entire construct is placed within a silicone cover. A schematic of the sensor function is shown in Figure B.2. Pressure applied to the sensor changes the amount of light detected by the sensor which is proportional to the pressure applied. This sensor, however, is quite thick as compared to earlier mentioned commercially available resistive sensor options.

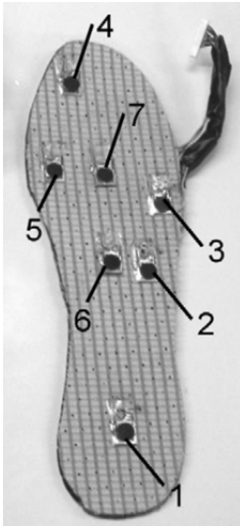

Figure B.1. PSCR used as an insole for measuring plantar pressures. The numbers 1-7 denotes the seven sensor systems placed on the insole [42]

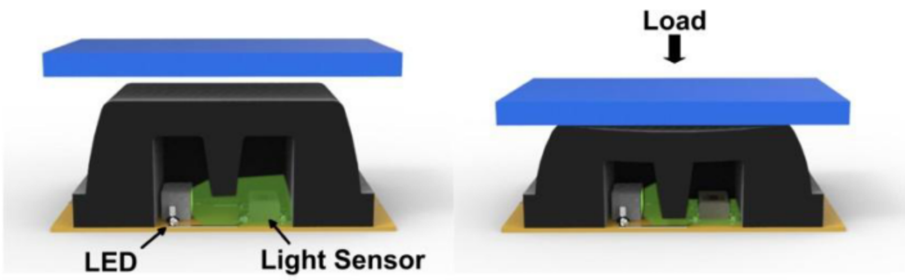

Figure B.2. Functioning of an optoelectronic sensor. An LED emits light that is blocked when a load is applied to the sensor. The percentage of light blocked is relative to the pressure applied on the system [43]

The advantage of using an insole over a force plate or motion capture is its portability. Several commercial systems also allow plug and play options, drastically reducing the setup time required. Pressure insoles are also actively used for improving running, and sport training. Owing to its lightweight and easy to slip on and use nature, it could be a potential wearable system for people with disabilities.

Appendix C. Design of Linear Regression Model

A linear regression model is a linear relation between an output and several inputs. Least squares is used to estimate the weights or coefficients of each input towards the prediction of output. In this study, Linear Regression Model was created using MATLAB^{TM}. A *fitlim* command was used. The inputs were the plantar pressure from the pressure insole, and the targets were forces and moments in 3D. Coefficients are assigned to each plantar pressure sensor data. Additionally, an intercept is added to the predictive model to correct for bias. *fitlim* assigns the coefficients that best fit the relation between input and output. A few sensors are weighted to zero, if they do not contribute significantly to the prediction of the output.

A total of 6 models were created for each foot. This includes a dedicated model for forces and moments in the X, Y, and Z axis. A typical model used in this study can be written as follows in Equation C.1.

$$Force_{LZ} = Intercept + Coeff1 * (sensor1) + Coeff2 * (sensor2) + ...$$
$$... + Coeff151 * (sensor151) \tag{C.1}$$

The Equation C.1 provides the force in the Z axis for the left leg, given the plantar pressure from the 151 insole sensors. *Coeff* denotes the weights given to each sensor and Intercept is a scalar bias added to the model. This model can predict quiet standing, initiation of walking, cyclical walking and deceleration of walking. Similarly, coefficients are generated for the forces and moments in 3D.

A representative model for the prediction of vertical force on the left leg for subject 9 is described here. The weights in Table C.1 show the contribution of each sensor to the output force. It is seen that sensors 1, 2, 3, and 4 are given zero weights, and can be ignored for predicting the output.

Table C.1. Coefficients of the model for estimating the vertical force on the left foot for subject 9.

Sensor	Coeff	Sensor	Coeff	Sensor	Coeff	Sensor	Coeff
Intercept	20,17	39	-0,76	78	2,07	117	1,89
1	0,00	40	-1,24	79	0,44	118	-8,74
2	0,00	41	1,09	80	2,89	119	-1,23
3	0,00	42	-0,89	81	3,89	120	-2,46
4	0,00	43	3,23	82	15,13	121	0,52
5	1,11	44	1,74	83	-1,73	122	-5,42
6	-0,17	45	-0,48	84	0,96	123	8,18
7	-2,35	46	-33,76	85	-11,66	124	2,64
8	-0,49	47	-0,26	86	6,70	125	-2,36
9	0,06	48	-1,78	87	-2,30	126	-2,24
10	-4,07	49	1,67	88	8,64	127	-0,63
11	1,02	50	-0,51	89	-5,24	128	4,10
12	-1,07	51	-0,02	90	2,12	129	3,13
13	0,37	52	-0,75	91	3,32	130	7,70
14	0,38	53	-1,85	92	-9,61	131	-0,05
15	1,26	54	-0,29	93	-1,43	132	-0,37
16	-0,26	55	0,33	94	0,44	133	1,19
17	2,27	56	2,21	95	1,11	134	1,00
18	3,63	57	0,60	96	-9,88	135	1,36
19	-0,40	58	6,73	97	-2,19	136	-4,46
20	16,99	59	1,94	98	2,50	137	0,94
21	-0,43	60	-3,26	99	2,45	138	-0,83
22	-0,19	61	0,50	100	-2,61	139	-2,33
23	-0,98	62	0,23	101	1,66	140	2,55
24	-1,81	63	-2,24	102	7,00	141	-2,64
25	-2,90	64	-2,83	103	6,72	142	-5,33
26	2,27	65	-0,98	104	0,76	143	4,71
27	-1,53	66	-1,10	105	2,44	144	-0,01
28	-2,02	67	-4,26	106	8,26	145	2,99
29	-0,07	68	2,28	107	-4,27	146	2,24
30	-1,84	69	-1,11	108	-12,62	147	-0,31
31	1,19	70	0,45	109	-13,17	148	0,95
32	-6,05	71	-0,85	110	9,95	149	-0,67
33	2,75	72	0,07	111	-0,22	150	1,12
34	2,85	73	-1,37	112	0,27	151	-3,78
35	0,64	74	-0,01	113	-5,83		
36	-0,95	75	1,20	114	-0,28		
37	2,04	76	25,24	115	3,33		
38	2,42	77	-1,61	116	-2,10		

Appendix D. Additional graphs

Additional graphs are displayed in this section.

Appendix D.1. Fused $\mathbf{x}_{CoM}$

The position of CoM from the two stages are fused to get the fused $\mathbf{x}_{CoM}$. The position estimated from the predicted and measured 3D forces and moments are compared here.

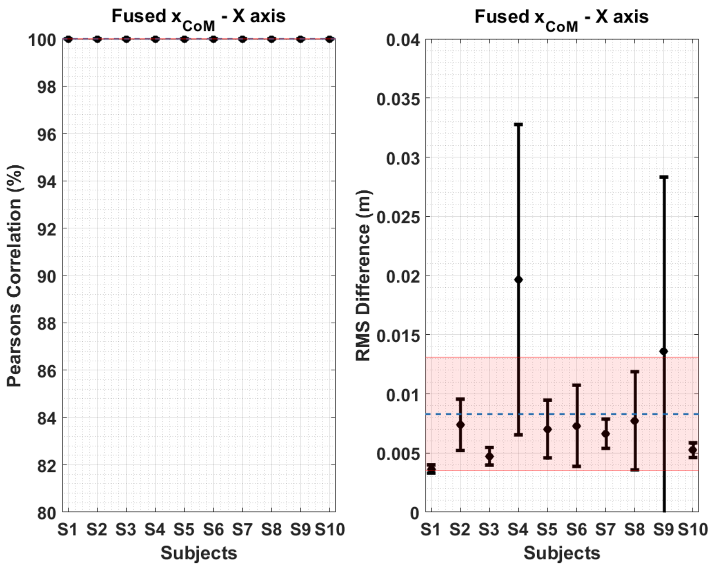

Figure D.1. (**a**) Pearson's Correlation and (**b**) RMS of the differences for the fused $\mathbf{x}_{CoM}$ in the X axis. The mean of the values for each subject is depicted as filled circles with an error bar that denotes its standard deviation. The horizontal blue dashed line and light red region shows the mean and standard deviation of the measurements among all subjects respectively.

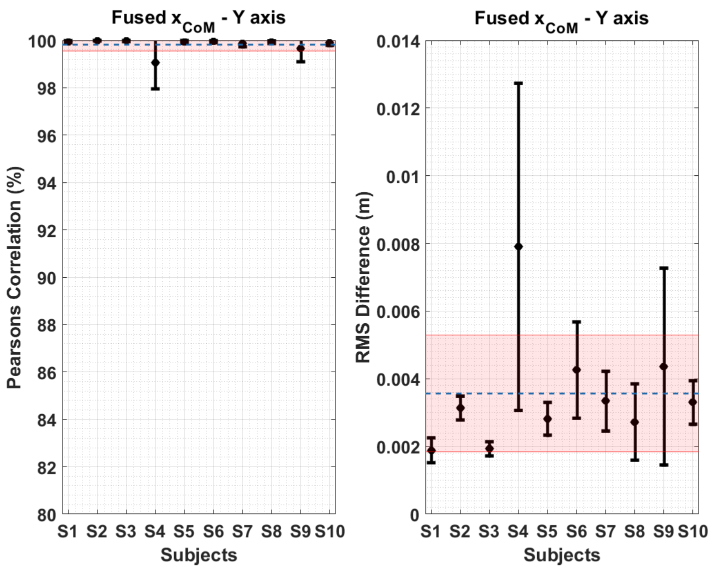

Figure D.2. (**a**) Pearson's Correlation and (**b**) RMS of the differences for the fused $\mathbf{x}_{CoM}$ in the Y axis. The mean of the values for each subject is depicted as filled circles with an error bar that denotes its standard deviation. The horizontal blue dashed line and light red region shows the mean and standard deviation of the measurements among all subjects respectively.

Appendix D.2. RMS of absolute differences for $\mathbf{x}_{CoM}$ *Stages 1 and 2*

The position of CoM from the two stages are compared between the estimations from predicted and measured 3D forces and moments. The absolute value of the RMS of the differences are displayed.

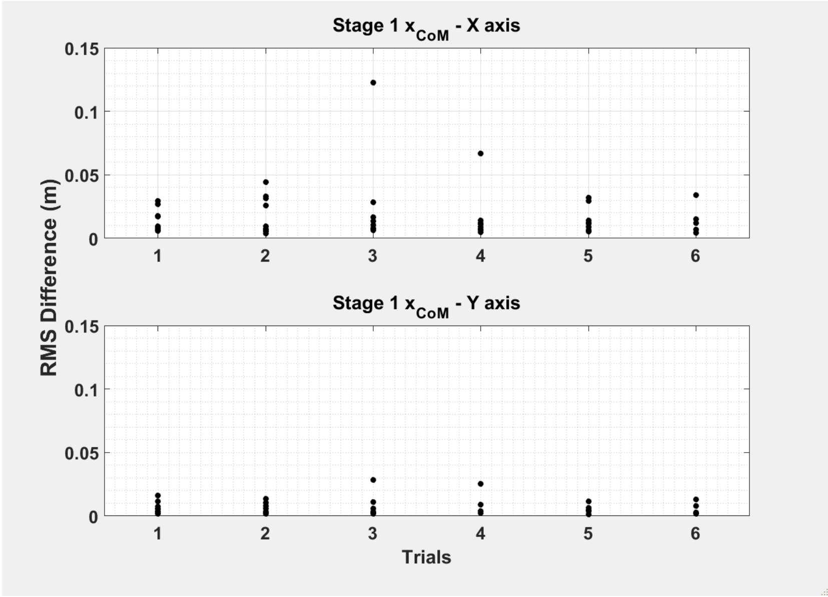

Figure D.3. RMS of the differences between the Stage 1 $\mathbf{x}_{CoM,S1}$ from predicted and measured 3D forces/moments in (**a**) X and (**b**) Y axis. Each dot represents the RMS of difference for one walking trial for a subject. The graph is a cluster plot of all walking trials of all subjects.

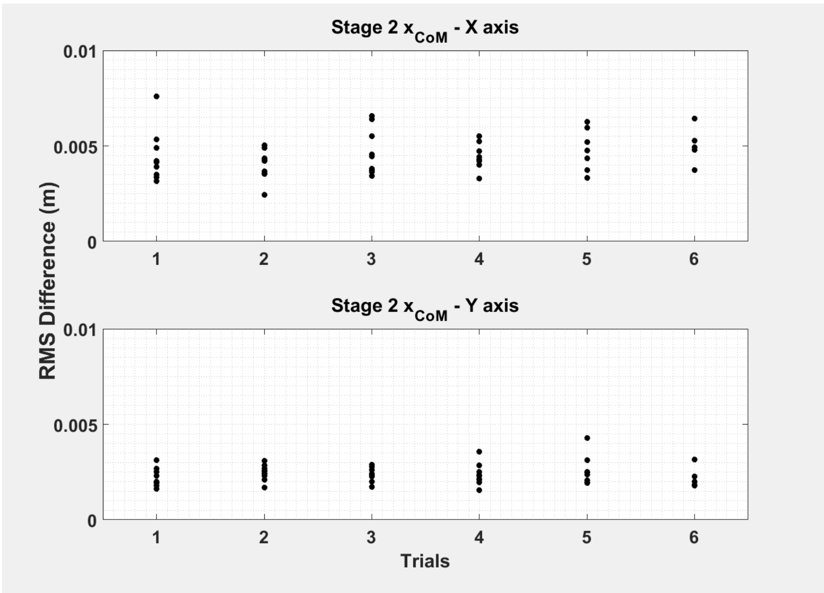

Figure D.4. RMS of the differences between the Stage 2 $\mathbf{x}_{CoM,S2}$ from predicted and measured 3D forces/moments in (**a**) X and (**b**) Y axis. Each dot represents the RMS of difference for one walking trial for a subject. The graph is a cluster plot of all walking trials of all subjects.

Appendix E. Derivatives of the confusion matrix

In addition to the descriptives of the confusion matrix described in Equation 9, other derivatives are calculated for this studied in this section. TP denotes True positives and TN denotes True Negatives. TP and TN refers to the sample points rightly classified as unstable and stable respectively by the DSM estimated from the predicted 3D forces/moments respectively. FP (False Positives) and FN (False Negatives) denote the sample points falsely classified as unstable and stable respectively by the DSM estimated from the predicted 3D forces/moments. In the confusion matrix in Table 2, TP = 2831, TN = 14797, FP = 140 and FN = 139. Other derivatives are described and shown in Table E.1.

Table E.1. Complete list of derivatives obtained from the confusion matrix

Derivative	**Formula**	**Value %**
Sensitivity	TP/P	95.3
Specificity	TN/N	99.1
Precision	TP/(TP+FP)	95.3
Negative Predictive Value	TN/(TN + FN)	99.1
Fall Out	FP/N	0.9
False Discovery Rate	FP/(TP + FP)	4.7
Accuracy	(TP + TN)/(TP + FP + FN + TN)	98.4
F1	2TP/(2TP + FP + FN)	95.3

References

1. Tyson, S.F.; Hanley, M.; Chillala, J.; Selley, A.; Tallis, R.C. Balance disability after stroke. *Physical therapy* **2006**, *86*, 30–38.
2. Kwakkel, G.; Kollen, B.; Lindeman, E. Understanding the pattern of functional recovery after stroke: facts and theories. *Restorative Neurology and Neuroscience* **2004**, *22*, 281–299.
3. Balasubramanian, C.K.; Neptune, R.R.; Kautz, S.A. Variability in spatiotemporal step characteristics and its relationship to walking performance post-stroke. *Gait and Posture* **2009**, *29*, 408–414.
4. van Asseldonk, E.H.F. Restitution and compensation in the recovery of function in the lower extremities of stroke survivors. PhD thesis, University of Twente, 2008.
5. World Health Organization. Towards a Common Language for Functioning , Disability and Health ICF. *International Classification* **2002**, *1149*, 1–22.
6. Dobkin, B.H. Rehabilitation after stroke. *New England Journal of Medicine* **2005**, *352*, 1677–1684.
7. Veltink, P.H.; Liedtke, C.; Droog, E.; Van Der Kooij, H. Ambulatory measurement of ground reaction forces. *IEEE Transactions on Neural Systems and Rehabilitation Engineering* **2005**, *13*, 423–427.
8. Weenk, D.; Roetenberg, D.; van Beijnum, B.J.F.; Hermens, H.; Veltink, P.H. Ambulatory Estimation of Relative Foot Positions by Fusing Ultrasound and Inertial Sensor Data. *IEEE transactions on neural systems and rehabilitation engineering* **2014**, *4320*, 1–10.
9. Schepers, H.M.; Koopman, H.F.J.M.; Veltink, P.H. Ambulatory assessment of ankle and foot dynamics. *IEEE Transactions on Biomedical Engineering* **2007**, *54*, 895–902.
10. van Meulen, F.B.; Weenk, D.; Buurke, J.H.; van Beijnum, B.J.F.; Veltink, P.H. Ambulatory assessment of walking balance after stroke using instrumented shoes. *Journal of NeuroEngineering and Rehabilitation* **2016**, *13*, 48.
11. van Meulen, F.B.; Weenk, D.; van Asseldonk, E.H.F.; Schepers, H.M.; Veltink, P.H.; Buurke, J.H. Analysis of Balance during Functional Walking in Stroke Survivors. *Plos One* **2016**, *11*, 20.
12. Schepers, H.; van Asseldonk, E.; Buurke, J.; Veltink, P. Ambulatory Estimation of Center of Mass Displacement During Walking. *IEEE Transactions on Biomedical Engineering* **2009**, *56*, 1189–1195.
13. Liedtke, C.; Fokkenrood, S.A.W.; Menger, J.T.; van der Kooij, H.; Veltink, P.H. Evaluation of instrumented shoes for ambulatory assessment of ground reaction forces. *Gait and Posture* **2007**, *26*, 39–47.
14. Hof, A.L.; Gazendam, M.G.J.; Sinke, W.E. The condition for dynamic stability. *Journal of Biomechanics* **2005**, *38*, 1–8.
15. Karatsidis, A.; Bellusci, G.; Schepers, H.; de Zee, M.; Andersen, M.; Veltink, P. Estimation of Ground Reaction Forces and Moments During Gait Using Only Inertial Motion Capture. *Sensors* **2016**, *17*, 75.
16. Hegde, N.; Bries, M.; Sazonov, E. A Comparative Review of Footwear-Based Wearable Systems. *Electronics* **2016**, *5*, 48.
17. Abdul Razak, A.H.; Zayegh, A.; Begg, R.K.; Wahab, Y. Foot Plantar Pressure Measurement System: A Review. *Sensors* **2012**, *12*, 9884–9912.
18. Koch, M.; Lunde, L.K.; Ernst, M.; Knardahl, S.; Veiersted, K.B. Validity and reliability of pressure-measurement insoles for vertical ground reaction force assessment in field situations. *Applied Ergonomics* **2016**, *53*, 44–51.
19. Ma, C.; Wong, D.; Lam, W.; Wan, A.; Lee, W. Balance Improvement Effects of Biofeedback Systems with State-of-the-Art Wearable Sensors: A Systematic Review. *Sensors* **2016**, *16*, 434.
20. Forner Cordero, A.; Koopman, H.J.F.M.; Van Der Helm, F.C.T. Use of pressure insoles to calculate the complete ground reaction forces. *Journal of Biomechanics* **2004**, *37*, 1427–1432.
21. Savelberg, H.; de Lange, A. Assessment of the horizontal , fore-aft component of the ground reaction force from insole pressure patterns by using artificial neural. *Clinical Biomechanics* **1999**, *14*, 585–592.
22. Fong, D.T.P.; Chan, Y.Y.; Hong, Y.; Yung, P.S.H.; Fung, K.Y.; Chan, K.M. Estimating the complete ground reaction forces with pressure insoles in walking. *Journal of Biomechanics* **2008**, *41*, 2597–2601.
23. Rouhani, H.; Favre, J.; Crevoisier, X.; Aminian, K. Ambulatory assessment of 3D ground reaction force using plantar pressure distribution. *Gait & Posture* **2010**, *32*, 311–316.
24. Sim, T.; Kwon, H.; Oh, S.E.; Joo, S.B.; Choi, A.; Heo, H.M.; Kim, K.; Mun, J.H. Predicting complete ground reaction forces (GRFs) and moments (GRMs) during gait with insole plantar pressure information using a wavelet neural network. *Journal of biomechanical engineering* **2015**, *137*, 1–9.

25. Hof, A.L. Scaling gait data to body size. *Gait and Posture* **1996**, *4*, 222–223.
26. World Health Organisation. Cardiovascular Dieases. Available online : http://who.int/mediacentre/factsheets/fs317/en/.
27. WHO. Global status report on noncommunicable diseases 2014. *World Health Organisation* **2014**, p. 176.
28. National Institute of Neurological Disorders and Stroke. Introduction to Stroke. Available online : http://www.ninds.nih.gov/disorders/stroke/knowstroke.htm.
29. National Stroke Association. What is Stroke? Available online : http://www.stroke.org/understand-stroke/what-stroke.
30. Centraal Bureau voor de Statistiek. Deaths, underlying cause of death, 2016. Available online : http://statline.cbs.nl/statweb/publication/?vw=t{&}dm=slen{&}pa=7052eng.
31. Ritter, L.; Coull, B. Lowering the Risks of Stroke in Women (and Men), 2015. Available online : http://heart.arizona.edu/heart-health/preventing-stroke/lowering-risks-stroke.
32. National Stroke Association. Hemiparesis and Stroke. Available online : http://www.stroke.org/we-can-help/survivors/stroke-recovery/post-stroke-conditions/physical/hemiparesis.
33. Pollock, A.; Farmer, S.E.; Brady, M.C.; Langhorne, P.; Mead, G.E.; Mehrholz, J.; van Wijck, F. Interventions for improving upper limb function after stroke. *The Cochrane Library* **2014**, *11*, CD010820–CD010820.
34. Rehabilitation Institute of Chicago. Rehab Measures. Available online : http://www.rehabmeasures.org/default.aspx.
35. Braun, B.J.; Veith, N.T.; Hell, R.; Döbele, S.; Roland, M.; Rollmann, M.; Holstein, J.; Pohlemann, T. Validation and reliability testing of a new, fully integrated gait analysis insole. *Journal of foot and ankle research* **2015**, *8*, 54.
36. Howell, A.M.; Member, S.; Kobayashi, T.; Hayes, H.A.; Foreman, K.B.; Bamberg, S.J.M.; Member, S. Kinetic Gait Analysis Using a Low-Cost Insole **2013**. *60*, 3284–3290.
37. Kraus, A.; Odenwald, S. Determining Ground Reaction Forces Using a Pressure Distribution Measuring System (P156). *The Enginnering of Sport*, *2*, 111–116.
38. Barnett, S.; Cunningham, J.L.; West, S. A comparison of vertical force and temporal parameters produced by an in-shoe pressure measuring system and a force platform. *Clinical Biomechanics* **2001**, *16*, 353–357.
39. Moufawad el Achkar, C.; Lenoble-Hoskovec, C.; Paraschiv-Ionescu, A.; Major, K.; Büla, C.; Aminian, K. Instrumented shoes for activity classification in the elderly. *Gait and Posture* **2016**, *44*, 12–17.
40. Benocci, M.; Rocchi, L.; Farella, E.; Chiari, L.; Benini, L. A wireless system for gait and posture analysis based on pressure insoles and Inertial Measurement Units. *Pervasive Computing Technologies for Healthcare 2009 PervasiveHealth 2009 3rd International Conference on* **2009**, *13*, 1–6.
41. Takaya, M.; Inoue, K.; Higuchi, K. Pressure-sensitive conductive elastomer compound, 1992. Available online : https://www.google.com/patents/US5175214.
42. Saito, M.; Nakajima, K.; Takano, C.; Ohta, Y.; Sugimoto, C.; Ezoe, R.; Sasaki, K.; Hosaka, H.; Ifukube, T.; Ino, S.; Yamashita, K. An in-shoe device to measure plantar pressure during daily human activity. *Medical Engineering and Physics* **2011**, *33*, 638–645.
43. Crea, S.; Donati, M.; De Rossi, S.M.M.; Oddo, C.M.; Vitiello, N. A wireless flexible sensorized insole for gait analysis. *Sensors* **2014**, *14*, 1073–1093.